



A Safety Control Method of Car-Following Trajectory Planning Based on LSTM

Xingyu CHEN¹, Haijian BAI², Heng DING³, Jianshe GAO⁴, Wenjuan HUANG⁵

Original Scientific Paper
Submitted: 26 Oct. 2022
Accepted: 30 Mar. 2023

¹ chenxingyu@mail.hfut.edu.cn, School of Automotive and Transportation Engineering, Hefei University of Technology

² Corresponding author, baihaijian@hfut.edu.cn, School of Automotive and Transportation Engineering, Hefei University of Technology

³ dingheng@hfut.edu.cn, School of Automotive and Transportation Engineering, Hefei University of Technology

⁴ 14705695537@163.com, School of Automotive and Transportation Engineering, Hefei University of Technology

⁵ huangwenjuan@hfut.edu.cn, School of Automotive and Transportation Engineering, Hefei University of Technology



This work is licensed under a Creative Commons Attribution 4.0 International License

Publisher:
Faculty of Transport and Traffic Sciences,
University of Zagreb

ABSTRACT

This paper focuses on the potential safety hazards of collision in car-following behaviour generated by deep learning models. Based on an intelligent LSTM model, combined with a Gipps model of safe collision avoidance, a new, Gipps-LSTM model is constructed, which can not only learn the intelligent behaviour of people but also ensure the safety of vehicles. The idea of the Gipps-LSTM model combination is as follows: the concept of a potential collision point (PCP) is introduced, and the LSTM model or Gipps model is controlled and started through a risk judgment algorithm. Dataset 1 and dataset 2 are used to train and simulate the LSTM model and Gipps-LSTM model. The simulation results show that the Gipps-LSTM can solve the problem of partial trajectory collision in the LSTM model simulation. Moreover, the risk level of all trajectories is lower than that of the LSTM model. The safety and stability of the model are verified by multi-vehicle loop simulation and multi-vehicle linear simulation. Compared with the LSTM model, the safety of the Gipps-LSTM model is improved by 42.02%, and the convergence time is reduced by 25s.

KEYWORDS

car-following model; LSTM; Gipps model; safety control; potential collision point.

1. INTRODUCTION

The car-following (CF) model has been a popular research topic in the transportation field for many years. The first CF model was proposed by Pipes and Chandler [1], after which many scholars began to investigate the topic. CF models can be classified based on the model output type, including interval prediction, velocity prediction and acceleration prediction. Moreover, they can be categorised into parametric models and nonparametric models based on the implementation method. Parametric models propose a relationship between input and output through equations, whereas nonparametric models are often obtained by using machine learning to learn CF data.

G. F. Newell proposed a simple homogeneous road CF model, in which the following vehicle has the same following trajectory as the preceding vehicle except for the translation in space and time [2, 3]. The famous collision avoidance Gipps model is a velocity control model that assumes that the preceding vehicle will have another sudden braking acceleration, and the following vehicle can still maintain a safe stopping distance [4]. The optimal velocity model (OVM) was proposed as the hyperbolic tangent function of velocity with respect to spacing and obtained under traffic congestion [5]. The generalised force model (GFM) studied how to solve the unsafe situations that may occur in the CF model [6]. Based on this model, the intelligent driver model (IDM) proposed the relationship between the real spacing and the expected minimum spacing and verified

that the characteristics of the model under OCT were basically consistent with the real data [7]. Based on the GFM model, Rui Jiang also proposed a full velocity difference model (FVDM) to study the properties of the model through analytical and numerical analysis methods and found that the model can describe the phase change process of traffic flow and estimate the evolution process of traffic flow congestion [8]. Yong proposed an improved FVD model considering the two vehicles in the driver's field of view and the vehicle immediately behind them [9]. F. Zong proposed a mixed-flow vehicle CF model based on the FVAD model to describe the microscopic CF behaviour of conventional vehicles (RVs) and autonomous vehicles (AVs) [10]. Qin and Chandan have built some car-following models for CAV [11, 12].

This type of model is characterised by its ability to incorporate dynamic behaviour while maintaining a simple calculation method. However, the formula derivation often requires some degree of experience, and some models may need adjustments based on actual data. One limitation of this approach is that it may not capture the full complexity and intelligence of human driving behaviour. Previous research has attempted to address safety concerns associated with the traditional dynamic car-following models. In this paper, we aim to address safety concerns related to the use of the intelligent long short-term memory (LSTM) model for car following behaviour.

Over the past decade, the development of big data and machine learning has led to their application in various research fields, owing to their strong theoretical foundation and remarkable ability to learn from data. For instance, the National Highway Traffic Safety Administration launched the Next Generation Simulation (NGSIM) project in 2006, making available a dataset that many researchers have utilised to examine microscopic traffic behaviours. Yang employed the Gipps model in combination with this dataset to remove unsafe behaviours in trajectories and continuously improved the dataset to train a random forest model [13]. M. Zhou proposed a classic cyclic neural network model to learn human driving behaviour data, which resulted in a model that was closer to real data than other models, such as the intelligent driver model (IDM) [14]. Heng Ding developed a connected and automated vehicle (CAV) driving strategy considering multiple vehicles in front, utilising an upgraded Elman neural network (ENN) model optimised by the Sparrow search algorithm (SSA) and a time-varying weighted model combined with the classical CF model [15]. F. Hui proposed a trajectory prediction model based on deep encoder-decoder and deep neural network (DNN) to address issues related to low prediction accuracy, inability to predict for an extended period and single adaptability of road segments in traditional prediction models [16]. W. Lu suggested a deep integrated neural network (DENN) model, which improves the accuracy of urban traffic state prediction, forming virtual graphs of highly correlated road sections [17]. Huang employed a LSTM neural network model to verify its capability to reproduce the stop-and-go phenomenon [18]. W. Fang incorporated an attention mechanism in the long short-term memory network for short-term traffic flow prediction [19]. Wang proposed a short-term traffic flow prediction model that leveraged the attention mechanism and 1DCNN-LSTM network [20], which combines the time expansion of CNN with the long-term memory advantage of LSTM. While these models can learn from data, they are akin to black boxes, making it challenging to explain and optimise the models locally.

The Gipps model was selected as the kinematic-based CF model due to its proven collision avoidance ability in numerous studies [3, 13, 21] and excellent safety features. By combining the Gipps model with machine learning-based CF models, the safety of autonomous vehicles can be enhanced. The Gipps model employs a 'safe velocity' concept to prevent accidents, which depends on the distance and velocity of the preceding vehicle. A detailed description of the Gipps model can be found in the reference [3].

The CF data is a type of time-series data, for which LSTM models have demonstrated superior learning ability, higher prediction accuracy and a more precise description of driving behaviour when compared to other machine learning models [22]. Additionally, LSTM models have a unique forgetting gate mechanism, which theoretically allows them to consider over 1000-time steps of historical time-series data, similar to human memory. Previous studies have shown that LSTM models that consider driver memory effects can better replicate real following behaviour and traffic flow state [22, 23]. However, in the case of autonomous vehicles, it is not entirely safe for the LSTM model to learn human following behaviour completely. Such models may learn hazardous driving behaviour, which could result in potential safety issues.

In this paper, two datasets, namely Dataset 1 and Dataset 2, were used. In recent years, machine learning methods have become increasingly popular for learning CF models, as studies [22, 23] have shown that these

models can replicate human CF behaviour. However, these models face urgent safety issues, as their safety cannot be verified in the same way as parametric models. To address this issue, this paper attempts to combine the advantages of the safety verifiability of parametric models with the learning ability of machine learning models to develop new CF models. Building on prior research, we propose a Gipps-LSTM model that combines a kinematic CF model (Gipps) and a data-driven CF model (LSTM). The proposed model retains the fundamental features of the classical LSTM model, such as temporality, and learns the intelligent features of human driving behaviour. Additionally, the Gipps model, a collision avoidance safety verifiable model, is introduced to address the safety concerns associated with the LSTM model.

2. DATA PREPARATION

2.1 Data collection

This paper employs two distinct datasets, namely Dataset 1 and Dataset 2, which are illustrated in *Figure 1*. Dataset 1, also known as NGSIM, is freely available to download from the official website [20–29]. On the other hand, Dataset 2 is collected by UAV, and Simi Motion is utilised to extract the vehicle trajectory data from the video. The video is approximately 15 minutes long, and the length of the road segment is around 200 m. The recording was performed at 10:00 a.m. There are many types of traffic flows in the road segment, such as free-flowing, stop-and-go traffic flows etc., which can capture CF behaviours comprehensively. Dataset 1 is employed both as a training and testing set, while Dataset 2 is solely utilised as the testing set.

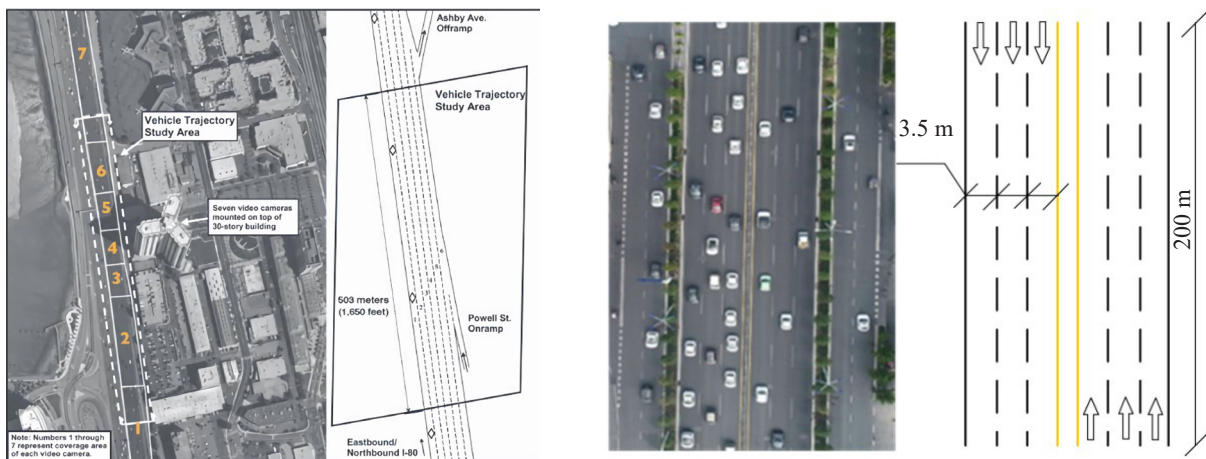


Figure 1 – Scenario of Dataset 1 (left) and Dataset 2 (right)

2.2 Data preprocessing

The difficulty to maintain a stable UAV position at high altitudes leads to errors in vehicle positioning in the video each time when extracting the video trajectory. Therefore, this paper adopts the sEMA method (Equations 1–3) to smooth the displacement trajectories of Dataset 2, and the velocity and acceleration are obtained from the first-order and second-order differences of the displacement trajectories [30].

Step 1: Use the symmetric exponential moving average (sEMA) to smooth the displacement trajectory data of the vehicle traveling from upstream to downstream of the road section.

Step 2: First-order difference and second-order difference are used to obtain the vehicle velocity and acceleration at each time step (0.1s).

Step 3: In steps 1 and 2 of smoothing the data, we will find that the velocity and acceleration of the processed data will change abruptly in the first and last small-time range. The reason for the sudden change is that the smoothing window for the first and last part of the data is relatively small, so the first and last second of the trajectory data of each trajectory should be excluded.

$$\bar{x}_\alpha(t_i) = \frac{1}{Z} \sum_{k=i-D}^{i+D} x_\alpha(t_k) e^{-|i-k|/\Delta} \tag{1}$$

$$Z = \sum_{k=i-D}^{i+D} e^{-|i-k|/\Delta} \tag{2}$$

$$\Delta = \frac{T}{dt} \tag{3}$$

Dataset 2 processed by this method is shown below. *Figure 2a* is the time-space diagram of vehicle trajectory in Dataset 2 after processing, which uses colour to distinguish the velocity of vehicles at different positions and at different times. *Figure 2b* shows the smoothed spacing and relative velocity scatter points. The spacing is mainly within 30 m, and the relative velocity is concentrated in (-2~2) m/s. *Figures 2c and 2d* show the time velocity diagram of a single vehicle, and the smoothing effect is closer to reality. It shows the acceleration time diagram of a single vehicle. It can be seen from the diagram that the acceleration value range is mainly between (-1~1) m/s².

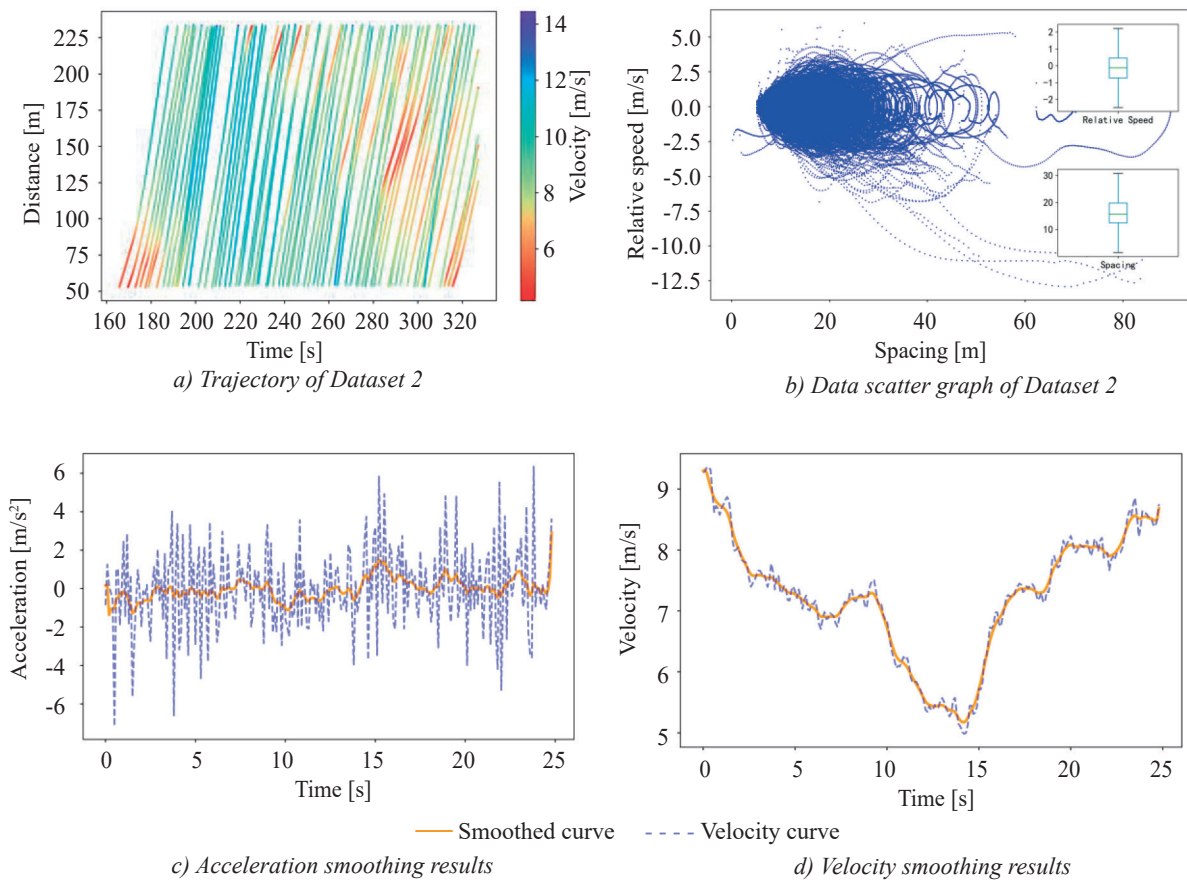


Figure 2 – Comparison between raw data and smoothed Dataset 2

3. MODEL

In this section we first train and test the LSTM CF model with the above two datasets and find that its simulated trajectory will have the problem of collision risk. To address this problem, we construct the Gipps-LSTM model by combining the LSTM model with the Gipps model and the concept of potential collision point.

Whether in a kinematic-based CF model or data-driven CF model, many scholars believe that the CF behaviour should be related to the spacing between the preceding and following vehicles, the relative velocity, the velocity of the following vehicle and the acceleration of the following vehicle. Therefore, in the classic LSTM and the modified LSTM (Gipps-LSTM) CF models in this article, the input variables are spacing $\Delta x_{n-1,n}(t)$ at time t , the relative velocity $\Delta v_{n-1,n}(t)$ and the following vehicle velocity $v_n(t)$, while the output is the acceleration $a_n(t+1)$ at time $t+1$ as shown in Equation 4.

$$a_n(t+1) = f(\Delta x_{n-1,n}(t), \Delta v_{n-1,n}(t), v_n(t)) \tag{4}$$

3.1 Limitations of the classical LSTM model

LSTM is able to handle data with time-series features, and training models using LSTM can fully learn the long-term dependencies in the training data. The output of the LSTM layer is shown in Equations 5–10 and the unit structure of the LSTM is shown in Figure 3.

1) Forget gate:

$$h_{t+1} = \sigma(W_{hx}x_{t+1}) + W_{ha}a_t + W_{hc}c_t + b_h \tag{5}$$

2) Input gate:

$$q_{t+1} = \sigma(W_{qx}x_{t+1}) + W_{qa}a_t + W_{qc}c_t + b_q \tag{6}$$

$$c_{t0} = \tanh(W_{cx}x_{t+1} + W_{ca}a_t + b_z) \tag{7}$$

3) Memory cell unit:

$$c_{t+1} = h_{t+1} \otimes c_t + q_{t+1} \otimes c_{t0} \tag{8}$$

4) Output gate:

$$o_{t+1} = \sigma(W_{dx}x_{t+1}) + W_{da}a_t + W_{dc}c_t + b_o \tag{9}$$

$$a_{t+1} = W_{ad}o_{t+1} + b_a \tag{10}$$

where $W_{hx}, W_{ha}, W_{hc}, W_{qx}, W_{qc}, W_{cx}, W_{qa}, W_{ca}, W_{dx}, W_{da}, W_{dc}, W_{ad}$ represents the weight matrix corresponding to each layer, b_h, b_q, b_z, b_o, b_a is the offset weight corresponding to each gate. And a_{t+1} is the predicted value of the acceleration of the model at the n^{th} vehicle at $t+1$.

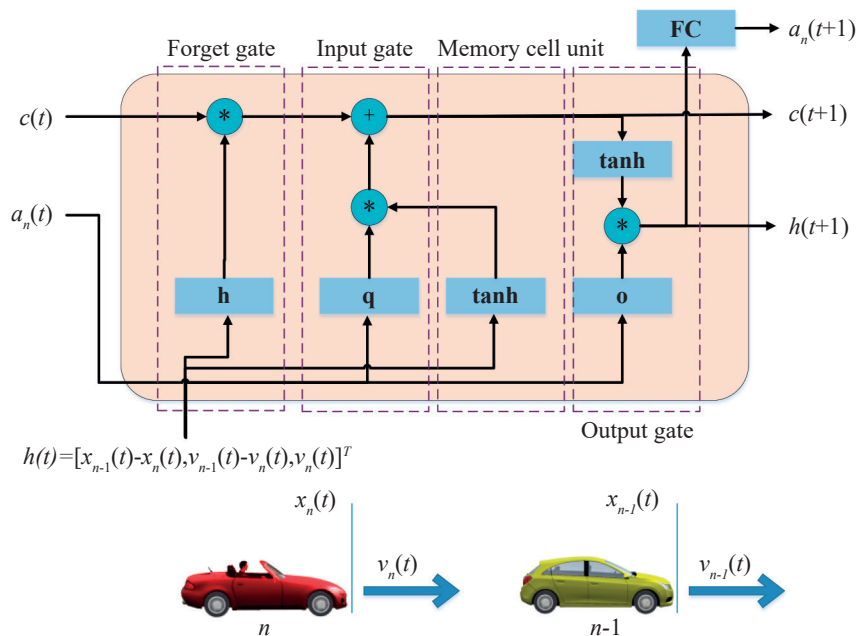


Figure 3 – LSTM unit structure diagram

The LSTM neural network model has a wide range of parameters and configurations, which include but are not limited to the activation function, loss function, optimisation algorithm, number of hidden layers, number of neural units per layer, learning rate, batch size and epoch. These parameters and configurations require ongoing adjustments to optimise the performance of the neural network. The loss function is an error function utilised to measure the disparity between the predicted value of the neural network and the actual value, with the *MSE* typically selected as the loss function. The specific formula for the *MSE* is presented in Equation 11.

$$MSE = \frac{1}{N} \sum_{n=1}^N \left(a_n^{sim} - a_n^{abs} \right)^2 \tag{11}$$

The findings of this study on the model training results for various combinations of hidden layers and neural units are presented in Figure 4a. The results indicate that a neural network with 2 hidden layers and 128 neural units per layer demonstrated the lowest model error, with training and testing errors being the closest. The plot

presented in Figure 4b illustrates the variation of the loss function during training and testing. The results show that an epoch value of 20 is sufficient. After conducting continuous testing and adjustment, the LSTM neural network structure was selected and utilised in subsequent simulation analyses. The chosen values for each parameter can be found in Table 1.

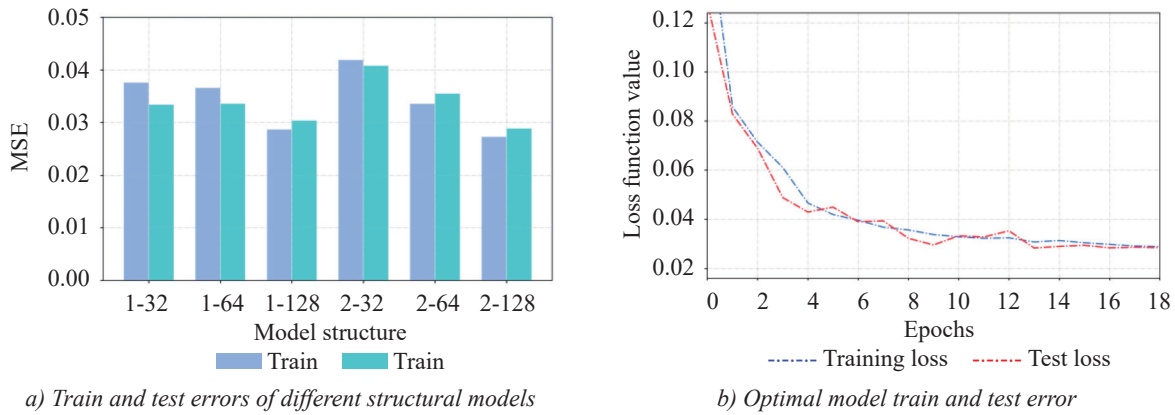


Figure 4 – Parameter adjustment

Table 1 – Parameter adjustment results of the LSTM CF model

| Parameter | Value | Parameter | Value |
|-------------------------|--------------|---------------|-------|
| Activation function | Sigmoid tanh | Learning rate | 0.001 |
| Loss function | MSE | Time step | 0.1s |
| Optimisation algorithm | Adam | Epoch | 20 |
| Number of hidden layers | 2 | Batch-size | 128 |
| Number of neural units | 128 | Dropout | 0.5 |

The LSTM model is simulated with the leading vehicle trajectory of the fleet in Dataset 1. The following vehicle trajectory is obtained by LSTM simulation acceleration under the premise of giving the position and velocity of the following vehicles at the initial moment. The simulation trajectory space-time diagram is shown in Figure 5.

In Figure 5a, the trajectory is generated using Dataset 1 with vehicle ID 1732 leading the way, and the classic LSTM model is used to simulate the nine trajectories followed. The initial velocity is the same as that of Dataset 1. In Figure 5b, a uniform distribution control error obeying [-0.5,0.5] is added to the simulation of Figure 5a to account for the inevitable vehicle control errors in real-world scenarios. The simulation results show that the model can adapt well to the adverse effects of this control error within a certain range, but it weakens the evacuation ability of traffic shock waves. These results indicate that the control error LSTM model is safe under normal conditions, but judging its absolute safety based on partial simulation trajectories is unreliable.

However, as shown in Figures 5c and 5d, when the leading vehicle is ID 1429, the LSTM model’s trajectory collides with the preceding vehicle. All following vehicles’ initial positions are initialised to be consistent with the data set. As the number of simulated vehicles increases, the following simulated vehicles also collide with the preceding vehicle. These results indicate that the model’s failure to learn the CF behaviour’s most important point is to stay safe, and thus the model requires modification.

3.2 Gipps-LSTM model

To address the issue of collision in LSTM, the present study proposes the Gipps-LSTM model, which combines the LSTM model and Gipps CF model. While the structure and parameter settings of the LSTM model have been previously introduced, this paper introduces the Gipps model, which provides a safe braking acceleration without considering the reaction time in the original model. The CF model is a dynamic system, and prediction models are established based on certain assumptions. Specifically, the Gipps model assumes that the preceding vehicle will decelerate at a_{n-1} until it stops to obtain a safe acceleration a_n , which is calculated through formulas using the most unfavourable assumption.

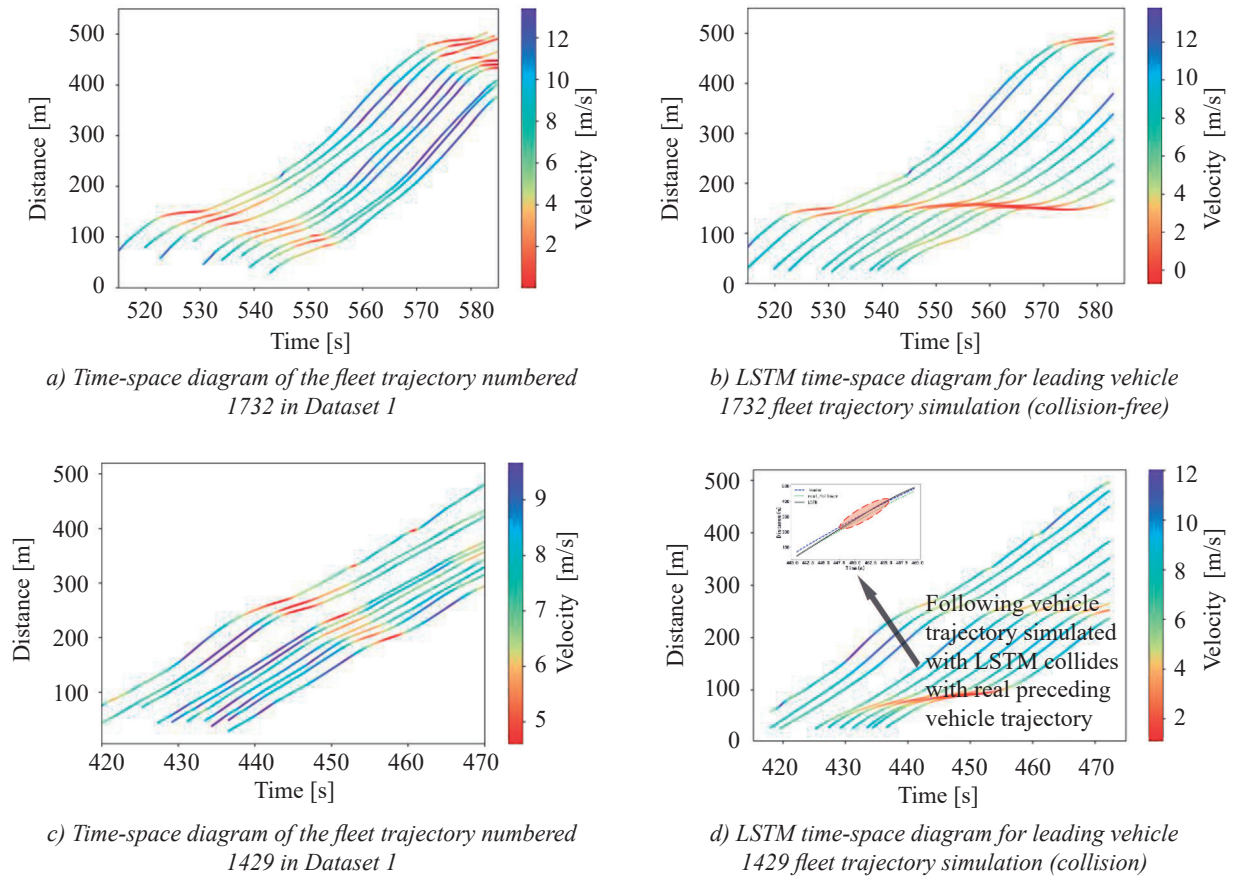


Figure 5 – LSTM trajectory simulation

The Gipps-LSTM model utilises the same unfavourable assumption, assuming that the preceding vehicle will decelerate until it stops, while the CF vehicle follows the vehicle using the LSTM model. If the following vehicle does not collide with the preceding vehicle when the velocity of the following vehicle is 0, the action taken can be fully referenced to the LSTM model. However, if a collision occurs, the LSTM model is considered a safety risk and the safe braking acceleration that needs to be taken must be calculated through a formula. By combining the collision avoidance advantage of the Gipps model and the superior ability of the LSTM model to fit sequence data, the new model is named the Gipps-LSTM model. Equations 5–10 present the LSTM model formula of the Gipps-LSTM model, while Equations 12–15 show some formulas of the Gipps model.

$$x_{n-1}^* = x_{n-1}(t) + \frac{v_{n-1}^2(t)}{2a_{n-1}} \tag{12}$$

$$x_n^* = x_n(t) + \frac{v_n^2(t)}{2a_n} \tag{13}$$

$$x_{n-1}^* - x_n^* \geq l_{n-1} \tag{14}$$

Putting Equations 12 and 13 into Equation 14, the following can be derived:

$$a_n \leq \frac{v_n^2(t)}{-\frac{v_{n-1}^2(t)}{a_{n-1}} + 2x_n(t) - 2x_{n-1}(t) + 2l_{n-1}} \tag{15}$$

where x_{n-1}^* represents the position where the preceding vehicle has been braking at the acceleration of a_{n-1} and will finally stop. x_n^* represents the position where the following vehicle brakes at the acceleration of a_n and finally stops. Equation 14 is to ensure that the spacing of the two vehicles is greater than the length of the preceding vehicle's body l_{n-1} when the two vehicles finally stop, and finally, the maximum value of the safe braking acceleration a_n of the CF vehicle in Equation 15 can be obtained.

Based on previous research [18-20], it has been discovered that the data-based CF model cannot verify safety through formulas directly. Furthermore, simulation results indicate that not all trajectories of the LSTM model can be maintained without collision. To address this issue, a virtual trajectory is constructed for the $(n-1)^{th}$ vehicle at each moment. Specifically, it is assumed that the $(n-1)^{th}$ vehicle brakes at that moment with a acceleration of a_{n-1} until it comes to a stop, while the LSTM model is used to simulate the following vehicle. If the spacing between two vehicles is greater than the length l_{n-1} of the preceding vehicle when both vehicles are at a final standstill, then the LSTM model is deemed safe at this moment. As the preceding vehicle decelerates to a stop, the LSTM model can control the following vehicle to stop before a collision occurs. However, if there is a potential collision risk at this moment, it is represented as α (Equation 16), and the moment $\alpha=1$ is referred to as the potential collision point (PCP).

$$\alpha = \begin{cases} 0, & \text{if } x_{n-1}^* - x_n^* \geq l_{n-1} \\ 1, & \text{else} \end{cases} \tag{16}$$

Based on this theory, the improved LSTM model proposed in this paper combines the characteristics of the safety verifiability of the formula and the characteristics of learning human driving data. It is ensured that the model can not only reproduce human intelligent driving behaviour, but also ensure safety. The final output formula of the model is as Equation 17.

$$a_n(t+1) = (1-\alpha)f(\Delta x_{n-1,n}(t), \Delta v_{n-1,n}(t), v_n(t)) + \alpha a_n \tag{17}$$

where a_n takes the maximum value of Equation 15; $f(\Delta x_{n-1,n}(t), \Delta v_{n-1,n}(t), v_n(t))$ is the output acceleration of the classic LSTM model. The Gipps-LSTM model is to use a formula to calculate the safe braking acceleration at a time when there is a potential risk of collision (at the time of $\alpha=1$) and adopt the acceleration to ensure the safety of the vehicle. The Gipps-LSTM safe trajectory decision-making method is shown in Figure 6.

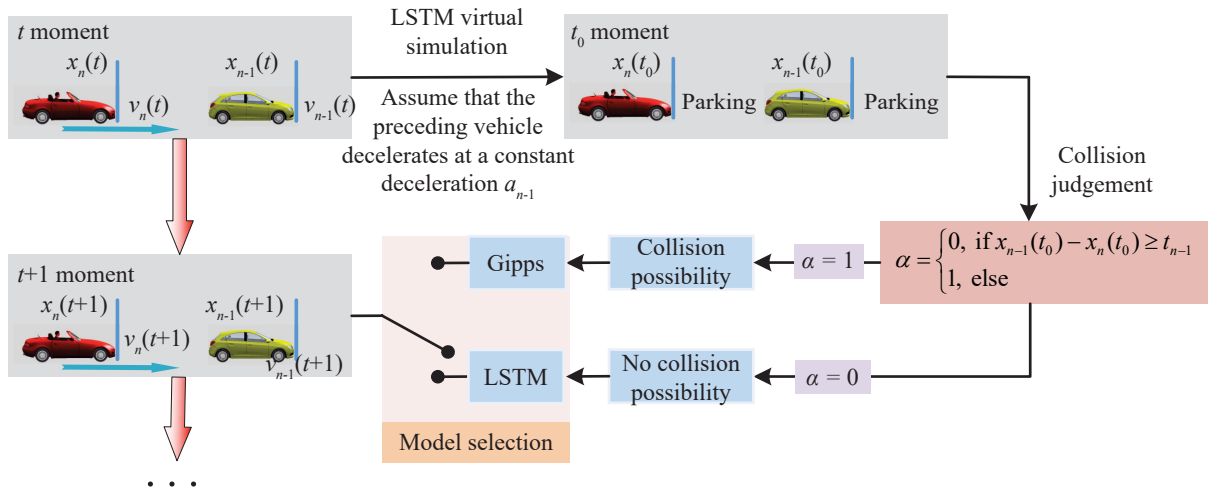


Figure 6 – the diagram flow of the Gipps-LSTM decision-making process

4. SIMULATION

4.1 Trajectory simulation

The main problem to be solved by this model is the trajectory collision problem that may occur in the simulation of the classic LSTM CF model. Therefore, in this paper, the classic LSTM model and the Gipps-LSTM model are simulated on the trajectory of Dataset 1 and Dataset 2 to compare the incidence of collisions. Due to the limited data extraction method, the length of the preceding vehicle is 5 m. This experiment is based on a computer with Intel Core i5-10400F and 16 GB of memory using Python 3.9, trained and run with the Keras framework in deep learning TensorFlow under the Jupyter Notebook development environment to implement Gipps-LSTM. The parameters in the Gipps-LSTM model were calibrated using the Genetic Algorithm (GA) library in Python. The objective function $U(s)$ is Equation 18. The performance indicator $RMSE_{(s,v,a)}$ is Equation 19, and the calibration results are shown for 20 percent of Dataset 1 and Dataset 2 in Table 2. The remaining 80 percent of Dataset 1 and Dataset 2 were used for simulation on Python. The simulation results are shown in Table 3.

$$U(s) = \frac{\sqrt{\frac{1}{T} \sum_{t=1}^T [s_{obs}(t) - s_{sim}(t)]^2}}{\sqrt{\frac{1}{T} \sum_{t=1}^T [s_{obs}(t)]^2} + \sqrt{\frac{1}{T} \sum_{t=1}^T [s_{sim}(t)]^2}} \tag{18}$$

$$RMSE_{(s,v,a)} = \sqrt{\frac{1}{T} \sum_{t=1}^T [(s, v, a)_{obs}(t) - (s, v, a)_{sim}(t)]^2} \tag{19}$$

Table 2 – Model calibration results

| Data | \bar{a}_{n-1} [m/s ²] | \overline{RMSE}_s [m] | \overline{RMSE}_v [m/s] | \overline{RMSE}_a [m/s ²] |
|-----------|-------------------------------------|-------------------------|---------------------------|---|
| Dataset 1 | -3.21 | 4.73 | 0.39 | 0.17 |
| Dataset 2 | -3.61 | 2.52 | 0.23 | 0.10 |

Table 3 – Model simulation collision rate

| Model | Data | Collision trajectory number | Total trajectory number | Collision rate (%) |
|--------------|-----------|-----------------------------|-------------------------|--------------------|
| Classic LSTM | Dataset 1 | 108 | 1029 | 10.5 |
| | Dataset 2 | 75 | 625 | 12 |
| Gipps-LSTM | Dataset 1 | 0 | 1029 | 0 |
| | Dataset 2 | 0 | 625 | 0 |

Although it is not possible to present the simulation effect of all trajectories, an example is provided to illustrate the effectiveness of the proposed method. Specifically, the braking trajectory of the leading vehicle (Vehicle No. 1023) is shown in Figure 7. Figure 7a presents the trajectory diagram of the simulation using the LSTM model. As shown, the traditional LSTM model will collide under the trajectory of the preceding vehicle, even if the initial state is relatively safe. In contrast, Figure 7b uses the Gipps-LSTM model to simulate the trajectory diagram. The Gipps-LSTM model can identify dangerous states and take safe operations, although it may slightly sacrifice efficiency. It is worth noting that efficiency and safety are incompatible, and to enhance safety, efficiency must be reduced. Thus, it is reasonable to reduce efficiency to obtain higher safety.

The classic LSTM model will collide with the preceding vehicle using part of Dataset 2 trajectory for simulation, highlighting the shortcomings of the pure LSTM model. Furthermore, machine learning models are not as interpretable as formula models, and mathematical formula derivation cannot be used to verify whether the model is entirely safe. Therefore, the proposed model in this article combines the collision avoidance advantages of the Gipps model to compensate for the limitations of the LSTM model.

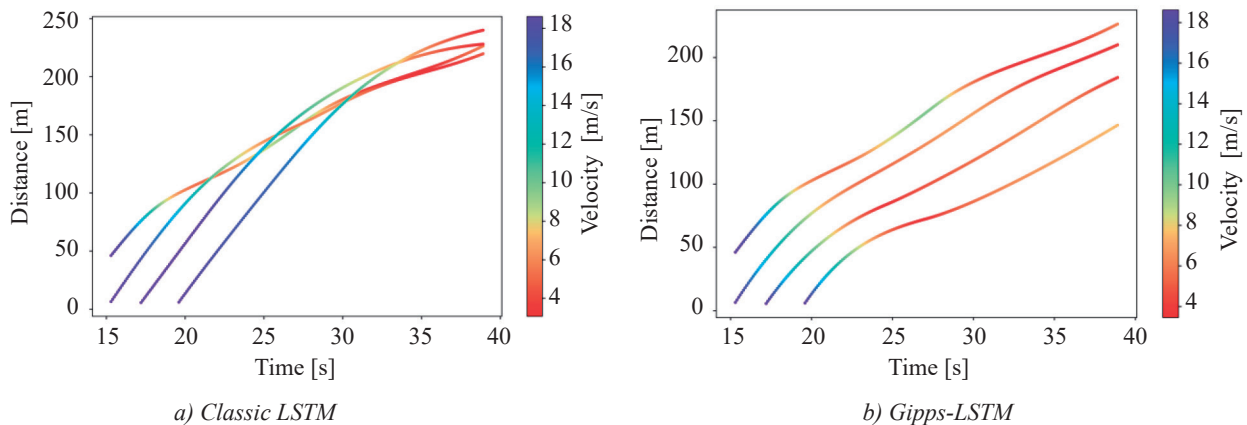


Figure 7 – Simulation comparison under different preceding vehicle accelerations

In this section, we compare the safety of the Gipps-LSTM model and the LSTM model simulated trajectories in scenarios with the different accelerations of the preceding vehicle. *Figure 8* shows the acceleration of the preceding vehicle set to -3, -4, -5, -6 m/s², respectively. As the braking velocity increases, the potential collision point (PCP) shows a downward trend. The reason is that the control of the Gipps model will ensure a safer spacing between the preceding and following vehicles. The result can be seen in *Figure 8*.

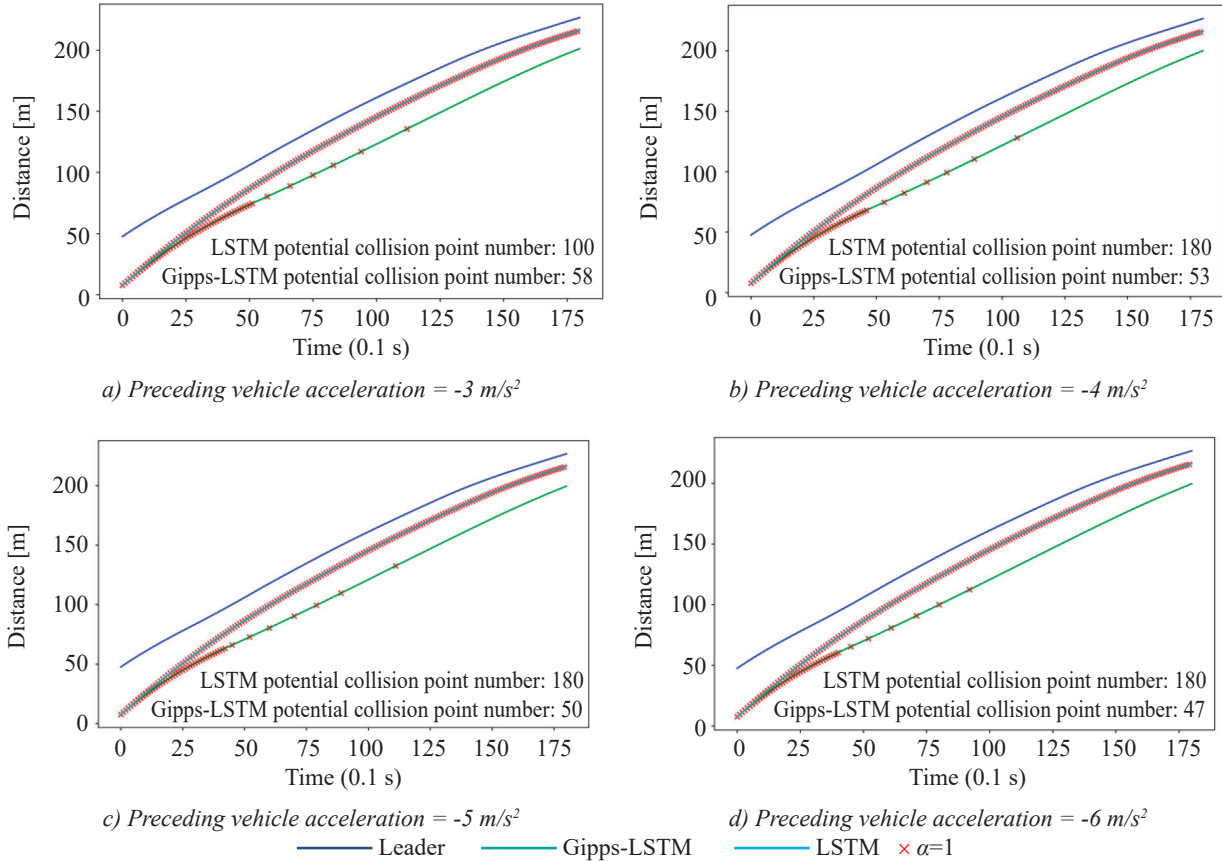


Figure 8 – Simulation comparison under different preceding vehicle accelerations

The simulation assumes that the braking acceleration of the preceding vehicle is 3, -4, -5, and -6 m/s², representing different degrees of danger in emergency situations, and is used to analyse the model’s simulation effect under various risk states. As shown in *Figure 8*, the calculated value of α for each moment of the LSTM model is equal to 1, indicating a potential collision risk at each moment. If the simulation continues in this state, the LSTM model will collide with the preceding vehicle.

In contrast, the Gipps-LSTM model can ensure that no collision occurs first and foremost, and secondly, the PCP value is significantly smaller than that of the LSTM model. Although the Gipps-LSTM model also calculates the PCP, the model has adopted the safe braking acceleration of the Gipps model, rendering the trajectory entirely safe. Moreover, from the perspective of PCP distribution under dangerous trajectories, the model will activate Gipps model control at the beginning stage, so that the Gipps model is rarely activated after the vehicle reaches a safer state. Therefore, the two control measures will not frequently switch, avoiding the problem of reduced vehicle comfort.

As depicted in *Figure 8*, the Gipps-LSTM model always maintains the same efficiency as the LSTM model when driving in a relatively safe environment. Hence, it can be concluded that the Gipps-LSTM model only sacrifices part of the efficiency during unsafe moments to enhance safety. When driving in a relatively safe environment, high efficiency is pursued similar to the LSTM model.

4.2 Multi-vehicle loop simulation

From the simulation in 4.1, the classical LSTM model used in single-lane multi-vehicle simulation has very unstable traffic flow characteristics. For example, the velocity will increase indefinitely, and collisions with the preceding vehicle will also occur in the simulation. *Figure 9a* is a simulation time-space diagram of a

Gipps-LSTM model with a simulation length of 1km for a single lane and a simulation duration of 200 seconds. Compared to the LSTM model, the velocity and spacing of the traffic flow are relatively stable under the simulation of the Gipps-LSTM model. The red area in *Figure 9a* is the set initial velocity of the fleet. From *Figure 9a*, the velocity of the fleet will continue to increase and then stabilise near a value, indicating that the model can intelligently adjust different densities. Velocities increase the efficiency of traffic flow. *Figure 9b* is the density-flow diagram of the Gipps-LSTM model traffic flow simulation. The traffic flow under this model is relatively close to the discontinuous curve model. The pre-congestion ($K < 79$) density-flow relationship exhibits a quadratic function, which is in excellent agreement with the existing traffic flow theory. *Figure 9c* shows the final stabilisation velocity of each vehicle in the traffic flow under the condition of setting different initial simulation velocities. The traffic flow will stabilise at a certain velocity when the set traffic flow density is consistent.

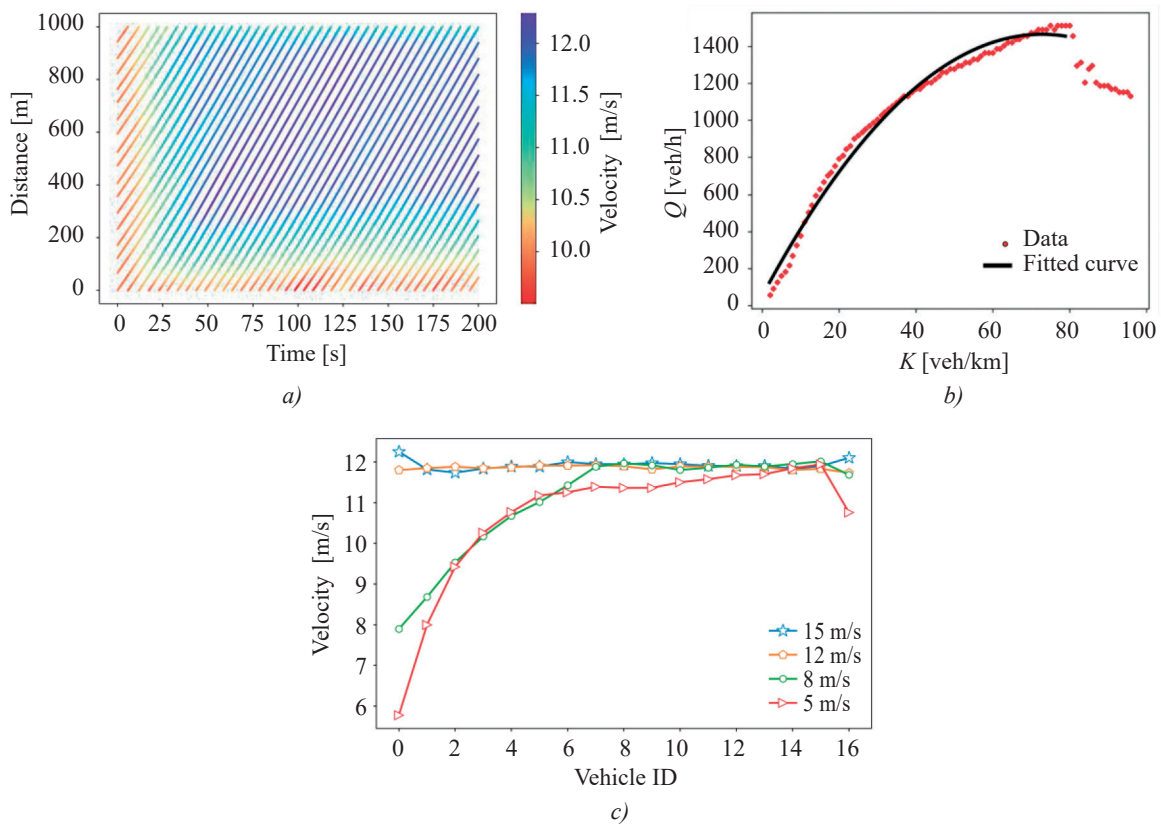


Figure 9 – a) Space-time diagram of traffic flow simulation based on Gipps-LSTM model (initial fleet velocity is 10 m/s), b) Time change curve of fleet velocity (vehicle density is 17 veh/km), c) Traffic flow simulation density-flow graph based on Gipps-LSTM model

When comparing the risks of the LSTM model and the Gipps-LSTM model, this paper chooses a more classic risk assessment index TTC (time to collision), and the TTC formula is as follows [31]:

$$TTC_n(t) = \frac{x_{n+1}(t) - x_n(t) - l}{v_n(t) - v_{n+1}(t)} \quad \forall v_n(t) - v_{n+1}(t) > 0 \quad (20)$$

Figure 10 displays the frequency diagram depicting the occurrence of time-to-collision (TTC) values lower than 10 in a single trajectory. As the TTC value decreases, the associated risk increases. This paper primarily investigates the performance of two models in scenarios where the risks are relatively high. The results in *Figure 10* indicate that, among all time steps where $TTC < 10$ in a single trajectory, the Gipps-LSTM model has a significantly higher mean value than the LSTM model. This observation demonstrates that the risk associated with the Gipps-LSTM model is considerably lower than that of the LSTM model.

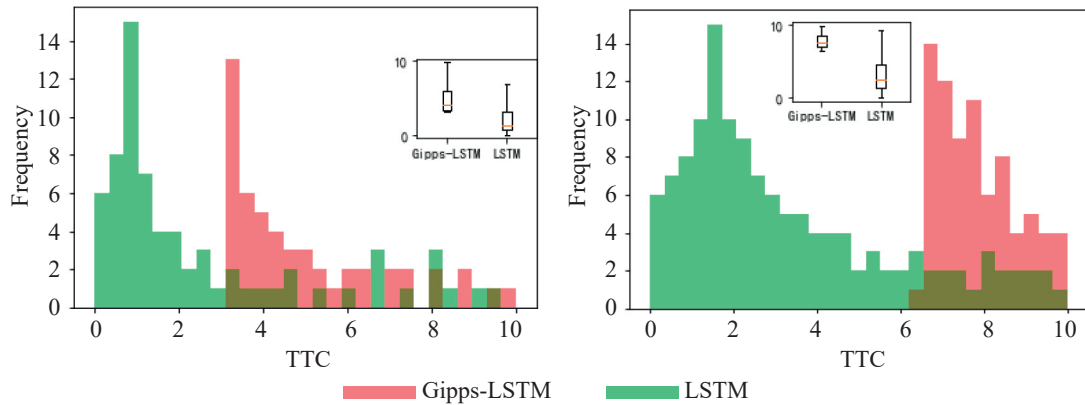


Figure 10 – Single trajectory TTC frequency

4.3 Multi-vehicle linear simulation

Based on the Gipps-LSTM model and LSTM model, the movement of multiple vehicles following each other is simulated, which is used to analyse the stability and safety of the following fleet. Set the driving state of the leading vehicle as to the following four parts [28]:

- 1) Driving for 50 s at a constant velocity of 5 m/s.
- 2) Accelerate for 10 s at an acceleration of 0.5 m/s².
- 3) Decelerate for 10 s at an acceleration of -0.5 m/s².
- 4) Driving 100 s at a constant velocity of 5 m/s.

In the simulation of fleet stability, the initial spacing of vehicles is set as 20 m and the vehicle length is 5 m. The initial velocity is set to 5 m/s, and the simulation time step to 0.1 s. Figure 11 shows the change in the velocity of ten following vehicles in the fleet with time. Assuming that the number of vehicles using the Gipps-LSTM model in the fleet is different, four different simulation results can be obtained. Table 4 shows the average TTC (TTC<10) and velocity of all vehicles in the fleet in the simulation time under the four simulation results, which are used to describe the safety and efficiency of the fleet.

Table 4 – Average TTC (TTC<10) and velocity of fleet simulation

| Number of Gipps-LSTM model | 0 | 3 | 6 | 9 (all) |
|----------------------------|---------|---------|--------|---------|
| Average TTC | 2.90529 | 3.12797 | 3.8038 | 4.12636 |
| Diff (%) | / | 7.66 | 23.12 | 7.16 |
| Average velocity [m/s] | 5.2924 | 5.2844 | 5.259 | 5.251 |
| Diff (%) | / | -0.15 | -0.48 | -0.15 |

In Figure 11, it can be observed that as the leading vehicle accelerates and then decelerates, the velocity of the follower also fluctuates, with both the LSTM and Gipps-LSTM models achieving stability after a period of time. The stability of the model is thus verified, and it is noteworthy that vehicles using the Gipps-LSTM model decelerate significantly faster than those using the LSTM model, as demonstrated in Figures 11b and 11c. Furthermore, as the proportion of vehicles using the Gipps-LSTM model increases in the fleet, the stable convergence velocity of the fleet is also improved. Specifically, when the entire fleet is simulated with the Gipps-LSTM model, the convergence velocity is improved by 50% compared to the simulation using the LSTM model, as shown in Figures 11a and 11d. Table 4 also shows that as the proportion of Gipps-LSTM model vehicles increases in the fleet, the average TTC of the fleet increases, indicating an overall improvement in the safety of the fleet. Notably, the average TTC value increases by 42.02% when the entire fleet is simulated with the Gipps-LSTM model, compared to when it is simulated with the LSTM model. However, the average vehicle velocity is only reduced by 0.79%, which suggests that the Gipps-LSTM model does not significantly impact the fleet’s efficiency while improving its overall safety.

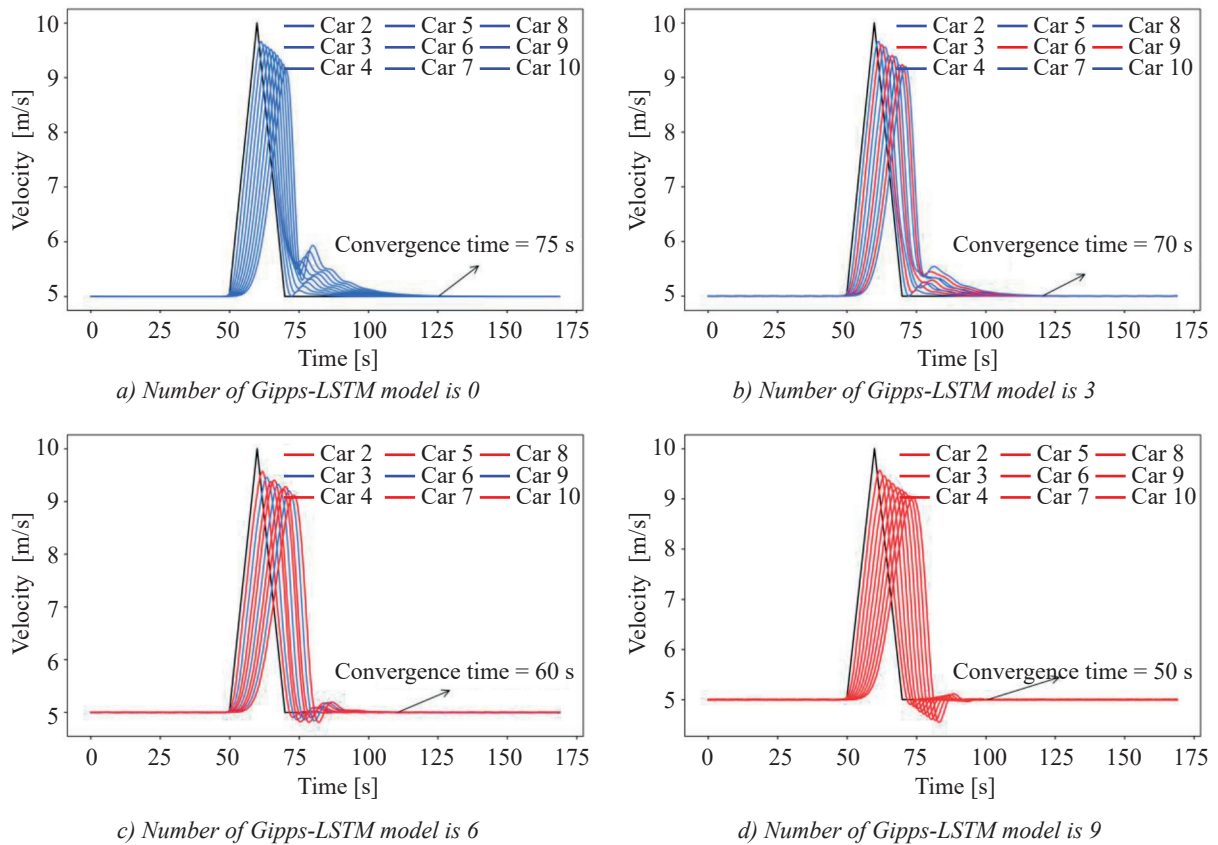


Figure 11 – Gipps-LSTM model (red) and LSTM (blue) model fleet simulation

5. DISCUSSION

In recent years, there has been an increasing interest in developing machine learning-based models for predicting CF behaviour in vehicles. While these models have shown promise in accurately predicting future vehicle positions, velocities and accelerations based on historical data, a key challenge is their safety verifiability. Machine learning-based models often lack interpretability, making it difficult to explain their decision-making processes, which is crucial for verifying their safety and reliability in autonomous vehicle operation. To solve this problem, the proposed a novel model, Gipps-LSTM, which combines the strengths of both machine learning and parametric models. However, there are some areas that require further investigation. Firstly, the Gipps-LSTM model is not sufficiently interpretable when applied to real-world scenarios. Secondly, the switching between the two control modes in the model can cause sudden acceleration under certain conditions, which reduces driving comfort. Finally, since there are two behaviours of car-following and lane-changing in real traffic flow, a single car-following model may not be enough to simulate the diversity of traffic behaviours, and finding internal connections between the two behaviours may be necessary.

6. CONCLUSION

In order to address the collision problem of some trajectories of the classic LSTM model, a new Gipps-LSTM model was developed by combining the LSTM model and the Gipps model. Through simulation tests, the following conclusions were drawn:

- 1) The Gipps-LSTM model has higher safety than the classic LSTM model, and the safety can be attributed to the Gipps model.
- 2) The PCP (probability of collision point) of the model will decrease instead of increasing as the dangerous situation becomes more urgent, which is related to the Gipps model’s role in adjusting the spacing at the beginning.
- 3) The velocity and spacing of the Gipps-LSTM model will be relatively stable in traffic flow simulation, and the basic traffic flow diagram can better match the existing traffic flow theory.

ACKNOWLEDGEMENTS

This work is supported by the National Natural Science Foundation of China (No.52072108), the Natural Science Foundation of Anhui Province (No.2208085ME148) and the Open Fund for State Key Laboratory of Cognitive Intelligence (No. W2022JSKF0504).

REFERENCES

- [1] Pipes LA. An operational analysis of traffic dynamics. *Journal of Applied Physics*. 1953;24(3):274-281. DOI: 10.1063/1.1721265.
- [2] Newell GF. A simplified car-following theory: A lower order model. *Transportation Research Part B: Methodological*. 2002;36(3):195-205. DOI: 10.1016/S0191-2615(00)00044-8.
- [3] Zhang W, et al. Asymmetric behaviour and traffic flow characteristics of expressway merging area in China. *Promet – Traffic&Transportation*. 2023;35(1):12-26. DOI: 10.7307/ptt.v35i1.4200.
- [4] Gipps PG. A behavioural car-following model for computer simulation. *Transportation Research Part B: Methodological*. 1981;15(2):105-111. DOI: 10.1016/0191-2615(81)90037-0.
- [5] Bando M, et al. Phenomenological study of dynamical model of traffic flow. *Journal De Physique I*. 1995;5(11):1389-1399. DOI: 10.1051/jp1:1995206.
- [6] Helbing D, Tilch B. Generalized force model of traffic dynamics. *Phys.Rev.E*. 1998;58(1):133-138. DOI: 10.1103/PhysRevE.58.133.
- [7] Treiber M, Hennecke A, Helbing D. Congested traffic states in empirical observations and microscopic simulations. *Phys.Rev.E*. 2000;62:1805-1824. DOI: 10.1103/physreve.62.1805.
- [8] Jiang R, Wu Q, Zhu Z. Full velocity difference model for a car-following theory. *Phys.Rev.E*. 2001;64(1 Pt 2):017101. DOI: 10.1103/PhysRevE.64.017101.
- [9] Peng Y, Liu S, Yu DZ. An improved car-following model with consideration of multiple preceding and following vehicles in a driver's view. *Physica A: Statistical Mechanics and its Applications*. 2020;538. DOI: 10.1016/j.physa.2019.122967.
- [10] Zong F, et al. Modeling AVs & RVs' car-following behavior by considering impacts of multiple surrounding vehicles and driving characteristics. *Physica A: Statistical Mechanics and its Applications*. 2022;589. DOI: 10.1016/j.physa.2021.126625.
- [11] Chandan K, Seco A, Bastos Silva A. A real-time traffic signal control strategy under partially connected vehicle environment. *Promet – Traffic&Transportation*. 2019;31(1):61-73. DOI: 10.7307/PTT.V31I1.2832.
- [12] Qin Y et al. Car-following model of connected cruise control vehicles to mitigate traffic oscillations. *Promet – Traffic&Transportation*. 2019;31(6):603-610. DOI: 10.7307/ptt.v31i6.2974.
- [13] D. Yang, et al. A novel car following control model combining machine learning and kinematics models for automated vehicles. *IEEE Trans. Intell. Transp. Syst.*. 2019;20(6):1991-2000. DOI: 10.1109/TITS.2018.2854827.
- [14] Zhou M, Qu X, Li X. A recurrent neural network based microscopic car following model to predict traffic oscillation. *Transportation Research Part C: Emerging Technologies*. 2017;84:245-264. DOI: 10.1016/j.trc.2017.08.027.
- [15] Ding H, et al. Driving strategy of connected and autonomous vehicles based on multiple preceding vehicles state estimation in mixed vehicular traffic. *Physica A: Statistical Mechanics and its Applications*. 2022;596:127154. DOI: 10.1016/j.physa.2022.127154.
- [16] Hui F, et al. Deep encoder–decoder–NN: A deep learning-based autonomous vehicle trajectory prediction and correction model. *Physica A: Statistical Mechanics and its Applications*. 2022;593. DOI: 10.1016/j.physa.2022.126869.
- [17] Lu W, et al. Traffic speed forecasting for urban roads: A deep ensemble neural network model. *Physica A: Statistical Mechanics and its Applications*. 2022;593. DOI: 10.1016/j.physa.2022.126988.
- [18] Huang X, et al. A car following model considering asymmetric driving behavior based on long short-term memory neural networks. *Transportation Research Part C: Emerging Technologies*. 2018;95:346-362. DOI: 10.1016/j.trc.2018.07.022.
- [19] Fang W, et al. Attention meets long short-term memory: A deep learning network for traffic flow forecasting. *Physica A: Statistical Mechanics and its Applications*. 2022;587 DOI: 10.1016/j.physa.2021.126485.
- [20] Wang K, et al. A hybrid deep learning model with 1DCNN-LSTM-Attention networks for short-term traffic flow prediction. *Physica A: Statistical Mechanics and its Applications*. 2021;583:126293. DOI: 10.1016/j.physa.2021.126293.
- [21] Treiber M, Kesting A. *Traffic Flow Dynamics*. 2013. p. 181-202.

- [22] Bai HJ, et al. Modeling differential car-following behavior under normal and rainy conditions: A memory-based deep learning method with an attention mechanism. *Chinese Physics B*. 2022.
- [23] Wang X, et al. Long memory is important: A test study on deep-learning based car-following model. *Physica A: Statistical Mechanics and its Applications*. 2019;514:786-795. DOI: 10.1016/j.physa.2018.09.136.
- [24] Punzo V, Montanino M. Do we really need to calibrate all the parameters? Variance-based sensitivity analysis to simplify microscopic traffic flow models. *IEEE Trans. Intell. Transp. Syst.* 2015;16(1):184-193. DOI: 10.1109/TITS.2014.2331453.
- [25] Shi K, et al. An integrated car-following and lane changing vehicle trajectory prediction algorithm based on a deep neural network. *Physica A: Statistical Mechanics and its Applications*. 2022;599. DOI: 10.1016/j.physa.2022.127303.
- [26] Zhang X, et al. Simultaneous modeling of car-following and lane-changing behaviors using deep learning. *Transportation Research Part C: Emerging Technologies*. 2019;104:287-304. DOI: 10.1016/j.trc.2019.05.021.
- [27] Xiao, et al. Capturing car-following behaviors by deep learning. *IEEE Transactions on Intelligent Transportation Systems*. 2017;19(3):910-920. DOI: 10.1109/TITS.2017.2706963.
- [28] Hui F, et al. Deep encoder–decoder–NN: A deep learning-based autonomous vehicle trajectory prediction and correction model. *Physica A: Statistical Mechanics and its Applications*. 2022;593. DOI: 10.1016/j.physa.2022.126869.
- [29] Ma L, Qu S. A sequence to sequence learning based car-following model for multi-step predictions considering reaction delay. *Transportation Research Part C: Emerging Technologies*. 2020;120. DOI: 10.1016/j.trc.2020.102785.
- [30] Thiemann C, Treiber M, Kesting A. Estimating acceleration and lane-changing dynamics from next generation simulation trajectory data. *Transportation Research Record*. 2008;2088(1):90-101. DOI: 10.3141/2088-10.
- [31] Jian M, Shi J. Analysis of impact of elderly drivers on traffic safety using ANN based car following model. *Safety Science*. 2020;122:104536. DOI: 10.1016/j.ssci.2019.104536.

陈星宇, 柏海舰, 丁恒, 高建设, 黄文娟

基于LSTM的汽车跟踪轨迹规划的安全控制方法

摘要:

本文主要研究深度学习模型产生的跟车行为中存在的碰撞安全隐患。在智能LSTM模型的基础上, 结合安全避撞的Gipps模型, 构建了一个新的模型Gipps-LSTM模型, 该模型不仅可以学习人的智能行为, 还可以保证车辆的安全。Gipps-LSTM模型组合的思路如下: 引入潜在碰撞点(PCP)的概念, 并通过风险判断算法控制和启动LSTM模型或Gipps模型。数据集1和数据集2被用来训练和模拟LSTM模型和Gipps-LSTM模型。仿真结果表明, Gipps-LSTM可以解决LSTM模型仿真中部分轨迹碰撞的问题。此外, 所有轨迹的风险水平都低于LSTM模型。该模型的安全性和稳定性通过多车循环仿真和多车线性仿真得到了验证。与LSTM模型相比, Gipps-LSTM模型的安全性提高了42.02%, 收敛时间缩短了25秒。

关键词:

跟驰模型; 长短时记忆; 吉普斯模型; 安全控制; 潜在碰撞点